AGU ADVANCING EARTH AND SPACE SCIENCE

Water Resources Research

RESEARCH ARTICLE
10.1029/2021WR031821

Estimating the Average River Cross-Section Velocity by Observing Only One Surface Velocity Value and Calibrating the Entropic Parameter

Farhad Bahmanpouri[1], Anette Eltner[2], Silvia Barbetta[1], László Bertalan[3], and Tommaso Moramarco[1]

[1]Research Institute for Geo-Hydrological Protection, National Research Council (CNR), Perugia, Italy, [2]Institute of Photogrammetry and Remote Sensing, Technische Universität Dresden, Dresden, Germany, [3]Department of Physical Geography and Geoinformatics, University of Debrecen, Debrecen, Hungary

Key Points:

- Applying the uncrewed aerial vehicle-based image acquisition technique to provide the maximum surface velocity
- Estimating the river discharge based on the Entropy concept relying on only maximum surface velocity
- Presenting cross-sectional velocity distribution calculated by the Entropy approach through European rivers, Sajó, and Freiberger Mulde

Supporting Information:

Supporting Information may be found in the online version of this article.

Correspondence to:

F. Bahmanpouri,
farhad.bahmanpouri@irpi.cnr.it

Citation:

Bahmanpouri, F., Eltner, A., Barbetta, S., Bertalan, L., & Moramarco, T. (2022). Estimating the average river cross-section velocity by observing only one surface velocity value and calibrating the entropic parameter. *Water Resources Research*, *58*, e2021WR031821. https://doi.org/10.1029/2021WR031821

Received 18 DEC 2021
Accepted 14 SEP 2022

Author Contributions:

Conceptualization: Farhad Bahmanpouri, Tommaso Moramarco
Data curation: Anette Eltner, László Bertalan
Formal analysis: Farhad Bahmanpouri, Tommaso Moramarco
Investigation: Farhad Bahmanpouri, Silvia Barbetta, Tommaso Moramarco
Methodology: Farhad Bahmanpouri, Silvia Barbetta, Tommaso Moramarco
Resources: Anette Eltner, László Bertalan
Supervision: Tommaso Moramarco
Validation: Farhad Bahmanpouri, Anette Eltner, Silvia Barbetta, László Bertalan, Tommaso Moramarco
Visualization: Farhad Bahmanpouri, Silvia Barbetta
Writing – original draft: Farhad Bahmanpouri, Anette Eltner

Abstract The current research aims to predict the velocity distribution and discharge rates in rivers based on the entropy concept using only one surface velocity measurement. In this direction, first, the uncrewed aerial vehicle (UAV)-based image acquisition technique was applied to collect the surface velocity distribution along two European rivers, the Sajó, and the Freiberger Mulde Rivers. Seven cross sections were chosen for the analysis. At each cross section, first, the entropic parameter $\Phi(M)$ was calibrated based on the maximum and mean velocity magnitudes, derived from Acoustic Doppler Current Profilers, respectively, showing a trend for all cross sections with a range of $0.6 < \Phi(M) < 0.75$. Next, the maximum surface velocity provided by the UAV was implemented as a single velocity input. Finally, the bathymetry data, herein collected by UAV, were considered as the input for the entropy approach. In this way, the entropy iterative method allowed estimating the mean flow velocity by identifying the location (dip) of maximum velocities across the river site and inferring the 2D velocity distribution. The results highlighted that the entropy approach can accurately predict the velocity distribution and discharge rates with a percentage error lower than 13%.

1. Introduction

Protecting and managing the waterways are of particular consequence in maintaining the balance between nature and human civilization. In this regard, river monitoring is one of the utmost issues in the field of river engineering due to (a) decision-making related to the protection of life and property from water-related hazards, such as floods, and (b) cost-effective management of freshwater that is safe and available for some applications, such as drinking, irrigation, energy, industry, recreation, and ecosystem health. Consequently, new technologies and methodologies are of particular importance to monitoring discharge rate considering various flow conditions at river gauges to improve the understanding of the surface hydrologic processes at the catchment scale (Tauro et al., 2014). Noncontact methods have been applied recently to measure flow properties, such as Doppler (velocity) radars (Fulton & Ostrowski, 2008; Moramarco et al., 2017; Welber et al., 2016) and large-scale particle image velocimetry (LSPIV; Fujita et al., 1998; Huang et al., 2018) or particle tracking velocimetry (PTV; Tauro & Salvatori, 2017; Tauro et al., 2014), applied to videos captured by cameras installed near the river. Nonetheless, these methods could be inefficient in some circumstances, for example, radar systems are not applicable during low flow conditions where velocity is less than 0.3 m/s or when the backscatter data pose systematic noise and the terrestrial camera systems require sufficient energy supply making them less feasible in isolated locations. Furthermore, the camera system relies on sufficient tracers at the river surface, good/stable lighting conditions, and in most cases, is not applicable during the night, unless extra equipment (NIR-light source) is installed and more specific processing is done. Tauro et al. (2018) addressed major image-based techniques that have been lately adopted within the hydrological research areas, including flow discharge estimation in riverine environments. The traditional techniques of flow characteristic measurements are relatively costly, time-consuming, and dangerous for operators especially during flood conditions, and further, they are not feasible in remote and inaccessible sections. Therefore, to overcome these challenges, first, uncrewed aerial vehicle (UAV) image-based methods can be used to record the surface velocity, and second, the entropy theory can be applied to turn the surface velocity into depth-averaged and cross-sectional velocity to derive the river discharge estimate. The potential of UAVs in hydrological sciences is vast (Acharya et al., 2021; Dal Sasso et al., 2021). Due to their flexible and facile

Writing – review & editing: Silvia Barbetta, László Bertalan, Tommaso Moramarco

usage, they are employed to measure river surface flow velocities (Eltner, Bertalan, et al., 2021) as well as the river bathymetry (Woodget et al., 2015), eventually allowing for the retrieval of river discharges by remote sensing (Eltner et al., 2020, Eltner, Mader, et al., 2021). UAV was applied for monitoring surface velocity through the radar sensor in some Alaska rivers where the surface velocity is assumed the maximum one (Fulton et al., 2020). The river surface flow velocities are measured using either LSPIV or PTV. Prior to any pattern or particle tracing, the captured images or video frames need to be coregistered to account for the movement of the UAV (Ljubičić et al., 2021). The stabilized image sequences are subsequently used to detect and track particles at the water surface. However, in many cases, the particles are not evenly distributed across the entire cross section, that is, faster flow in the main current and decreasing velocities outside, and therefore, hindering a reliable discharge retrieval by the velocity area method relying on depth-averaged velocity estimation if the range of given velocities is not captured.

The entropy concept has been vastly applied to predict the velocity distribution and other relevant parameters in open channel flow (Chiu, 1989; Chiu & Said, 1995; Chiu et al., 2005; Ebtehaj et al., 2018; Moramarco & Singh, 2010; Singh et al., 2017; Sterling & Knight, 2002; Termini & Moramarco, 2017). In terms of velocity estimation, the entropy concept can be applied to present cross-sectional velocity distributions in a given cross section of a river (Chiu, 1988; Singh, 2014). Moramarco and Singh (2010) and Moramarco et al. (2011) proposed the relations between entropic parameter and geometric and hydraulic characteristics of natural channels that affect the velocity profiles. Termini and Moramarco (2020) verified the feedback effect of cross-sectional flow on the longitudinal velocity distribution, suggesting that the location of dip represents the location where the maximum flow velocity occurs below the water surface. Chahrour et al. (2021) applied the entropy-based approach to discharge measurements for the gauging of the Isère River at the Grenoble University Campus based on an image-based technique. The particle tracking velocimetry (PTV) from video images was used to estimate surface velocities, which were considered as an input for the entropy approach. Recently, Bahmanpouri et al. (2022) applied the entropy approach using all surface velocity measurements collected by ADCP at cross sections in Amazon rivers. Their results highlighted that the entropy-based velocity distribution model can be used to predict the velocity field at confluences well enough to accurately estimate flow discharge despite the complex hydrodynamic settings.

Due to increasing flood disasters in recent years, simple, safe, and efficient procedures for estimating discharge and velocity rates are of particular demand. In this context, the combination of image-based technique and the entropy theory can be considered as one of the best solutions to meet these requirements. The present research aims, as a first attempt, to estimate the velocity and discharge rate in rivers applying the entropy concept relying only on a single maximum surface velocity measurement derived by UAV. This methodology is of particular benefit for measuring the flow discharge and velocity for rivers where there are difficulties of measurements by field devices during extreme flow conditions. In this regard, an inexpensive UAV-based remote sensing methodology was applied to collect the surface velocity distribution along two European rivers, the Sajó and the Freiberger Mulde Rivers, where concurrent ADCP measurements are also available. The novel contribution of the present work is proposing and testing a procedure to estimate the entropy-based discharge that (a) uses the maximum surface velocity as input and (b) considers the velocity dip to identify the possible maximum velocity below the water surface due to the existence of secondary currents. These two aspects make the difference with previous works (e.g., Chahrour et al., 2021; Fulton et al., 2020) where the surface velocity was assumed the maximum one without considering the possible presence of dip phenomenon. The entropic parameter Φ(M) was calibrated based on an intrusive approach, herein the maximum and mean velocity magnitudes of the ADCP data. This magnitude can be used for high flow conditions for the same transect. Next, at each cross section, the maximum surface velocity together with bathymetry data estimated from the UAV was considered as the input for the entropy approach. It should be mentioned that the bathymetry data derived from the UAV are in agreement with the bathymetry data recorded by ADCP with an acceptable accuracy as previously stated by researchers for river flow conditions (Bandini et al., 2018; Brasington et al., 2003; Kim et al., 2019; Rossi et al., 2020; Williams et al., 2013; Zinke & Flener, 2013) or near-shore shallow water conditions (Matsuba & Sato, 2018; Tsukada et al., 2020). The structure of the paper is as follows: Section 2 describes the field site and data collection; Section 3 presents the theoretical description of the entropy theory; Section 4 describes the results in terms of cross-sectional velocity distribution, discharge rate, and error analysis; the comparison of the vertical distribution of velocity between the entropy outputs and the available ADCP data is also presented. Section 5 outlines the final conclusions.

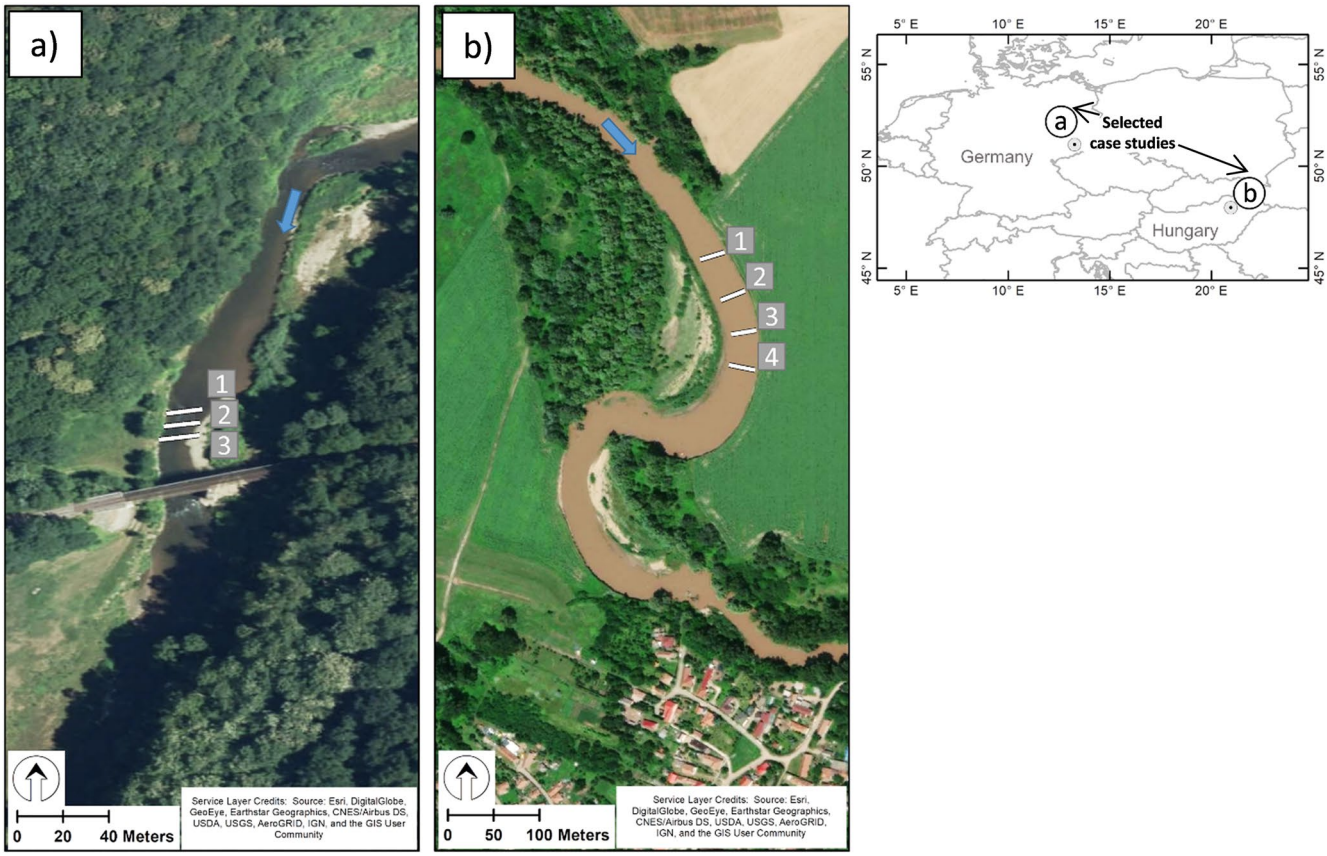

Figure 1. Location of the study areas: (a) Freiberger Mulde and (b) Sajó. The white lines represent the Acoustic Doppler Current Profilers reference cross section, while the blue arrow shows the main flow directions.

2. Field Site and Data Collection and Pre-Processing

UAV-based image acquisition was applied to collect the surface velocity distribution through two European rivers.

The Sajó River is transboundary flowing from the Eastern Carpathian ridges of Slovakia toward Hungary where it transforms into an alluvial type with the length of 124 km in Hungary. The basin size is 5,545 km^2 and the average discharge is around 24 m^3/s. The Sajó River has a mixed gravel-sand channel bed. However, the Hungarian section of the river has been engineered in several sub-reaches, but in the free-forming sections, it shows a meandering pattern (Bertalan et al., 2018, 2019). The observed river section exhibits high bank erosion rates revealing an unstable river bed and river topography. The Freiberger Mulde is the headstream of the river Mulde with a length of 124 km, whose catchment covers an area of 2,981 km^2 in the Czech Republic and Germany in central Saxony. It has a discharge rate of 35.3 m^3/s that is greater than that of the other headstream, the Zwickauer Mulde with a discharge rate of 26.4 m^3/s. The studied river reach is a natural river section and exhibits nonuniform flow conditions. Figure 1 shows the geographic details of these rivers. The Sajó and Freiberger Mulde Rivers have an average depth of 0.88 and 0.87 m, respectively, and a transect length of 27.5 and 16.7 m, respectively.

The UAV data were captured on a single day at each site. At the river Sajó in Hungary, the aircraft was slowly flown along the river reach continuously capturing a video, whereas the data were captured with the UAV hovering above the area of interest at flying heights of 35 (Sajó) and 30 m (Freiberger Mulde). The video lengths ranged between several minutes at Sajó and a few seconds at the Saxon rivers. The frame rate was 50 fps for the former study site and 25 fps for the latter site. Table 1 presents the date of measurements for ADCP and UAV.

In all the cases, the UAV video frames needed to be stabilized according to the approach explained in Eltner et al. (2020). Thereby, stable areas outside the river were used to orient all frames to the first video frames such

Table 1
Field Data Measurements by Acoustic Doppler Current Profilers and Uncrewed Aerial Vehicle

	Date of measurement	
Transect	ADCP	UAV
Sajó CS1	14.10.2019	14.10.2019
Sajó CS2	14.10.2019	14.10.2019
Sajó CS3	14.10.2019	14.10.2019
Sajó CS4	14.10.2019	14.10.2019
Freiberger Mulde CS1	26.10.2016	7.9.2016 (bathymetry), 26.10.2016 (surface flow velocity)
Freiberger Mulde CS2	26.10.2016	7.9.2016 (bathymetry), 26.10.2016 (surface flow velocity)
Freiberger Mulde CS3	26.10.2016	7.9.2016 (bathymetry), 26.10.2016 (surface flow velocity)

as they were all captured from the same perspective. Due to the movement along the river at Sajó, a further pre-processing step was necessary for selecting head frames in defined intervals and coregistering a specified number of subsequent tail frames to the headframe (Eltner, Bertalan, et al., 2021). The video frames were used to calculate the river topography and bathymetry as well as the flow velocities. The structure from Motion (SfM) photogrammetry (Eltner & Sofia, 2020) was used to retrieve the 3D geometry below and above the water surface. Due to the refraction impact that leads to an underestimation of water depth, the underwater points were corrected by the multiview refraction correction (Dietrich, 2017).

To estimate the flow velocities, the Good-Feature-To-Track method (Shi & Tomasi, 1994) was first used to detect particles at the water surface. Therefore, it was necessary to mask the water area, which was done by projecting the underwater 3D points into the image space to delineate the water region. The detected particles were then tracked by the Lucas Kanade optical flow algorithm (Lucas & Kanade, 1981), which performs a least squares matching by minimizing the pixel gray value differences between a template and the search region to find the new location of the particle. The final scaling of the velocity tracks was done by projecting the start and endpoint of each track through the projection center of the camera into the object space and intersecting the corresponding image ray with the water surface to retrieve the actual location of the track in 3D object space. The distance of the track was estimated and multiplied with the frame rate to eventually calculate the flow velocity. The reference flow velocity data were acquired with two ADCPs: a SonTek RiverSurveyor S5 in Hungary and a StreamPro from RDI in Germany. We have surveyed three cross sections at Freiberger Mulde and four cross sections at Sajó field sites, respectively. The post-processing method of the raw flow velocity data has been already described in Eltner, Mader, et al. (2021).

3. Theoretical Description

The distribution of velocity based on the entropy method along the verticals can be defined as

$$U(x_i, y) = \frac{U_{\max v}(x_i)}{M} \ln\left[1 + \left(e^M - 1\right)\frac{y}{D(x_i) - h(x_i)} \exp\left(1 - \frac{y}{D(x_i) - h(x_i)}\right)\right] \quad i = 1...N_v \tag{1}$$

where U is the time-averaged velocity, $U_{\max v}(x_i)$ is the maximum value of U along the ith vertical, x_i is the distance of the ith sampled vertical from the left bank, $h(x_i)$ is the dip, that is, the depth of $U_{\max v}(x_i)$ below the water surface, $D(x_i)$ the flow depth, y is the distance of the velocity point from the bed, and N_v is the number of verticals sampled across the river section. M is the entropic parameter and can be calculated using the linear entropic relation (Chiu, 1989; Moramarco et al., 2004):

$$U_m = \left(\frac{e^M}{e^M - 1} - \frac{1}{M}\right) U_{\max} = \phi(M) U_{\max} \tag{2}$$

$U_{\max}$ surmises the maximum value of $U_{\max v}(x_i)$ sampled in the cross-sectional flow area.

For a gauged river site, $\Phi(M)$ has been found to be constant for all flow conditions, while for ungauged sites, $\Phi(M)$ can be estimated as (Moramarco & Singh, 2010).

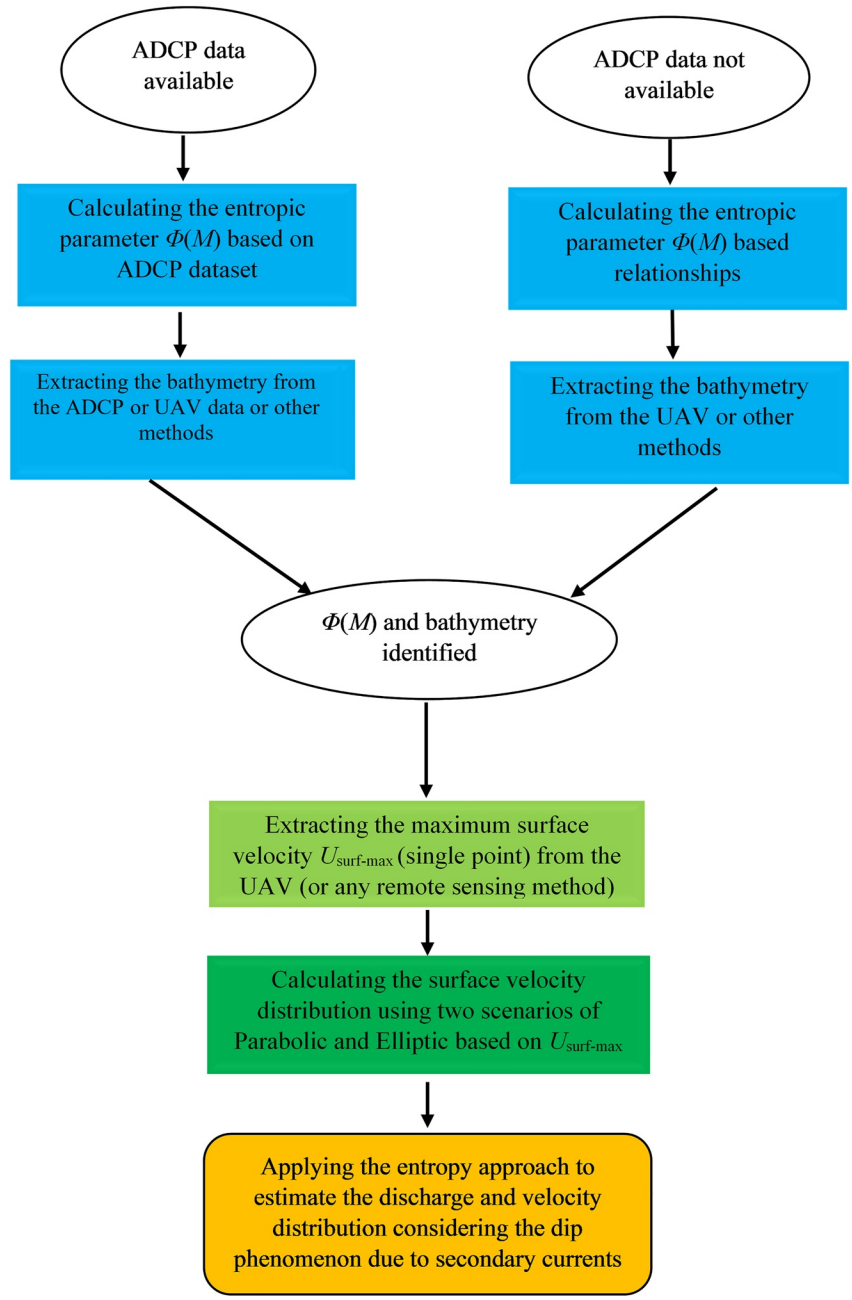

Figure 2. Flowchart of the procedure of applying the entropy method in the current research. The Acoustic Doppler Current Profilers data were available for the current research.

$$\phi(M) = \frac{\frac{1}{n}R^{1/6}/\sqrt{g}}{\frac{1}{k}\left[\ln\left(\frac{y_{max}}{y_o}\right) + \frac{h}{y_{max}}\ln\left(\frac{h}{D}\right)\right]} \tag{3}$$

where y_{max} is the location of U_{max} from the bottom and y_o is the datum where the velocity is equal to zero, k is the von Karman constant, R is the hydraulic radius ($R = A/P$, where A is the cross-sectional area of flow and P is its wetted perimeter), and D is the maximum flow depth.

If only surface velocities, $U_{surf}(x_i,D(x_i))$ are available at river site, then $U_{max}(x_i)$ can be estimated as (Fulton & Ostrowski, 2008)

Table 2
The Magnitudes of Φ(M) and M for the Selected Cross Sections Based on Acoustic Doppler Current Profilers Data

Transect	Observed mean velocity (m/s) (ADCP)	Observed maximum velocity (m/s) (ADCP)	Estimated maximum velocity (m/s) (entropy)	Φ(M)	M	Aspect ratio (width/depth)
Sajó CS1	0.82	1.12	1.11	0.732	3.24	26.4
Sajó CS2	0.69	1.14	1.13	0.605	1.30	33.3
Sajó CS3	0.65	1.06	1.05	0.613	1.40	29.6
Sajó CS4	0.98	1.35	1.25	0.726	3.12	37.5
FreibergerMulde CS1	0.57	0.93	0.88	0.611	1.37	18.4
FreibergerMulde CS2	0.65	0.97	0.82	0.668	2.17	18.6
FreibergerMulde CS3	0.68	1.14	0.98	0.678	1.16	20.2

$$U_{\max v}(x_i) = \frac{U_{\text{surf}}(x_i, D(x_i))}{\frac{1}{M}\ln\left[1 + (e^M - 1)\,\delta(x_i)\,e^{1-\delta(x_i)}\right]} \tag{4}$$

(where $\delta(x_i) = \frac{D(x_i)}{D(x_i)-h(x_i)}$. Specifically, if $h(x_i) = 0$, it follows $\delta(x_i) = 1$, and hence, $U_{\max v}(x_i) = U_{\text{surf}}(x_i, D(x_i))$. It is worth noting that the value of the maximum velocity is estimated by Equation 4 applying the procedure proposed by Moramarco et al. (2017), who, through an iterative approach, inferred the maximum velocity value changing the location of maximum velocity below the water surface. The location, known as dip, is identified by minimizing the error on M estimation. The distribution of the surface velocity in the entropy approach is based on either of the two scenarios of parabolic and elliptic that were developed by Corato et al. (2011).

4. Results and Discussion

This section is organized as follows: first, the calculation of the entropy parameter M for all cross-sections is presented; next, the results of the proposed procedure are presented for each cross section. The results comprise three parts (a) surface velocity by UAV compared to available near-surface ADCP velocity together with surface velocity distribution based on two scenarios of parabolic and elliptic distribution; (b) cross-sectional velocity distribution estimated by the entropy approach based on two scenarios of parabolic and elliptic distribution; (c) comparison between the estimated mean velocity and discharge by the entropy method and the available ADCP data. Figure 2 shows the flowchart of the procedure of applying the entropy method in the current research. Based

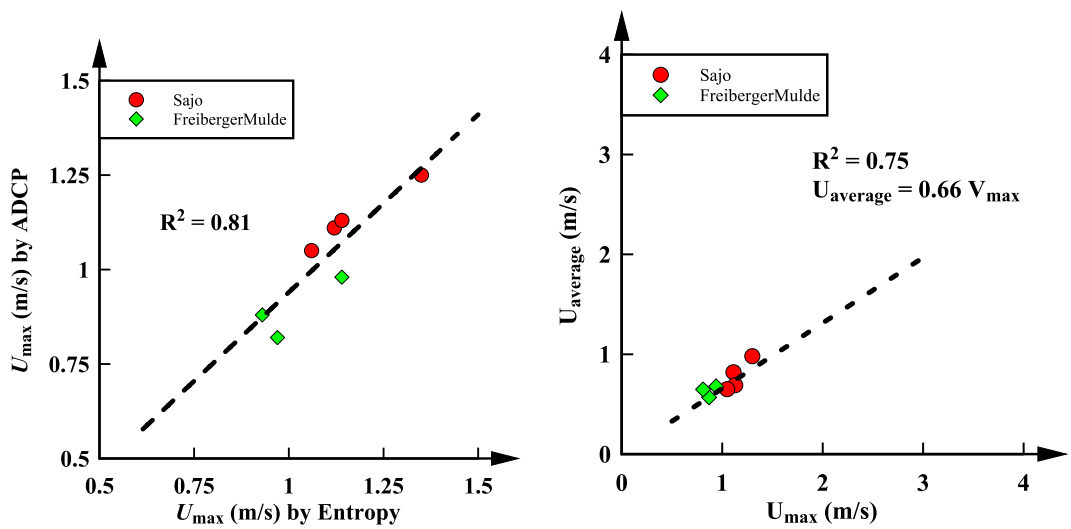

Figure 3. The correlation between velocity magnitudes. (a) Between maximum velocity by Entropy and Acoustic Doppler Current Profilers (ADCP) (b) Between maximum and average velocities by ADCP.

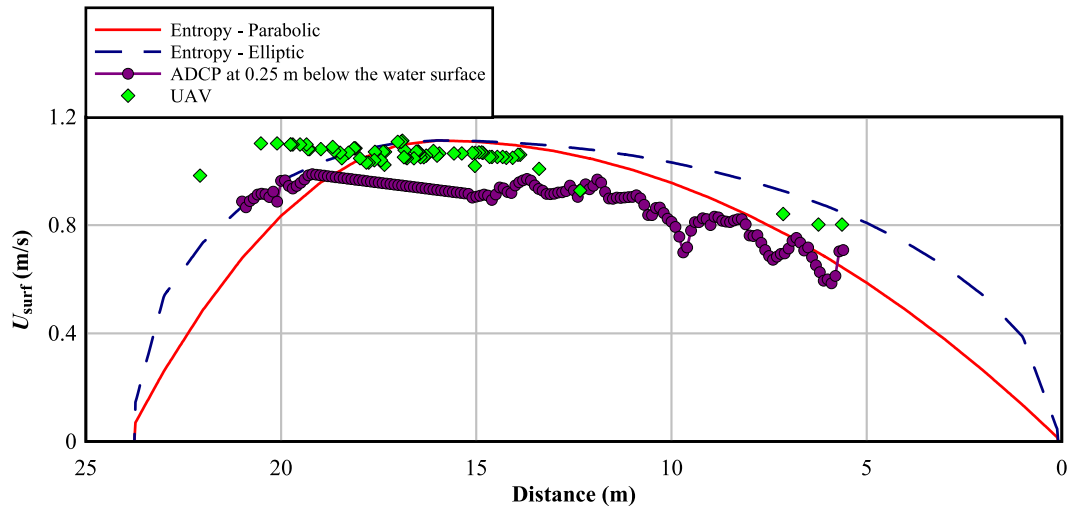

Figure 4. Surface velocity distribution based on Parabolic and Elliptic scenarios, Sajó CS1.

on the flowchart in Figure 2, there are two scenarios for calculating the entropic parameter: based on ADCP data where they are available and based on the relationship where there are no ADCP measurements. Then, the bathymetry data can be extracted based on ADCP or UAV data. Next, based on a single surface velocity collected by UAV or any remote sensing data, we can use two different scenarios of parabolic and elliptic distribution of surface velocity as input for the Entropy model. Finally, the discharge cross-sectional velocity by considering the velocity dip would be estimated using the Entropy approach.

4.1. Calculation of the Entropy Parameter

For the present data set, the magnitude of $\Phi(M)$ and M for the selected transects is listed in Table 2. The maximum velocity estimated by the entropy method, as calculated using Equation 4, also is added. A comparison between the observed and estimated maximum velocity magnitudes shows a fine agreement between the observed and estimated velocity data for Sajó River. The difference between the observed and estimated velocity data through the Freiberger Mulde River is mainly due to the difference between the surface velocity predicted by UAV (which is considered as the input for the entropy model) and the ADCP data with the maximum error percentage of 15% (for more details, see Eltner et al., 2020). Figure 3a shows the correlation between the maximum velocity observed by ADCP data and estimated by the entropy approach. Figure 3b highlights the correlation between maximum and mean velocity magnitudes as a description of $\Phi(M)$ where $\Phi(M) = U_m/U_{max.}$ Notably, U_{max} and U_m were derived from the ADCP measurements. Although the number of measurements in terms of pairs (U_m, U_{max}) is not enough, an overall idea of the dynamic of flow can be inferred. The entropic relation has been already tested and evaluated for many rivers and showed that the entropy parameter M is constant for gauged river sections (Corato et al., 2014; Xia, 1997). Therefore, M is fundamental to addressing velocity measurements during high floods when measurements can be conducted out only in the upper region of flow area where the maximum velocity U_{max} occurs (Moramarco & Singh, 2010). The magnitudes of $\Phi(M)$ for the present study were in agreement with the data reported for small rivers for example, $0.66 < \Phi(M) < 0.80$ for natural channels in the United States (Chiu et al., 2000), $0.6 < \Phi(M) < 0.68$ for Tiber River in Italy (Moramarco et al., 2019), $0.63 < \Phi(M) < 0.69$ for Godavari and Ulhas Rivers in India (Vyas et al., 2021), and for large rivers for example, $0.4 < \Phi(M) < 0.61$ for Amazon River in Brazil (Bahmanpouri et al., 2022). Also, $\Phi(M) = 0.88$ (Hii River data of Shinohara and Tsubaki (1959)) and $\Phi(M) = 0.91$ (Leo-River data of Leopold (1969)) were reported by Choo et al. (2011). The entropy parameter depends on both the suspended sediment rate and aspect ratio (flow width/flow depth). Greco and Moramarco (2016) based on field data at different river stations demonstrated that the entropic parameter changes with varying the aspect ratio but limited to the range of $0.5 < \Phi(M) < 0.8$. Nezu and Rodi (1986) and Vanoni (1941). Chiu et al. (2000) stated that the entropy concept takes a system view in which all factors, such as velocity distribution, discharge, sediment concentration, and roughness, slope, and geometrical shape of the channel, interact to maintain a

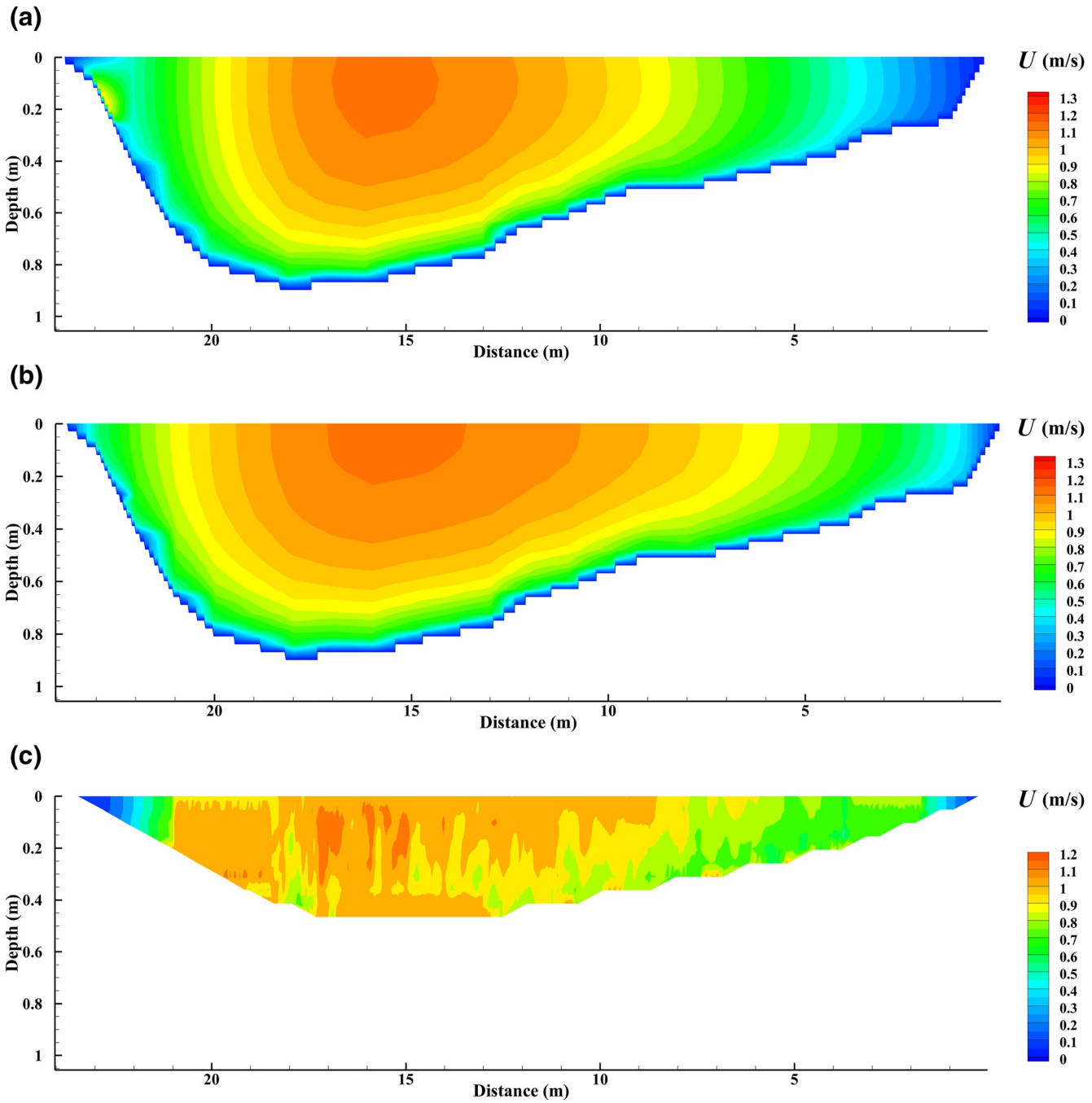

Figure 5. Cross-sectional velocity distribution, Sajó CS1 based on uncrewed aerial vehicle bathymetry.

Table 3
The Error Percentage for the Velocity and Discharge Rates

Transect	Scenario for the surface velocity distribution	Average velocity (m/s)		Velocity error (%)	Discharge (m^3/s)		Discharge error (%)
		Measured	Calculated		Measured	Calculated	
Sajó CS1	Parabolic	0.82	0.81	1.22	11.21	11.07	1.22
	Elliptic		0.87	6.10		11.89	6.10

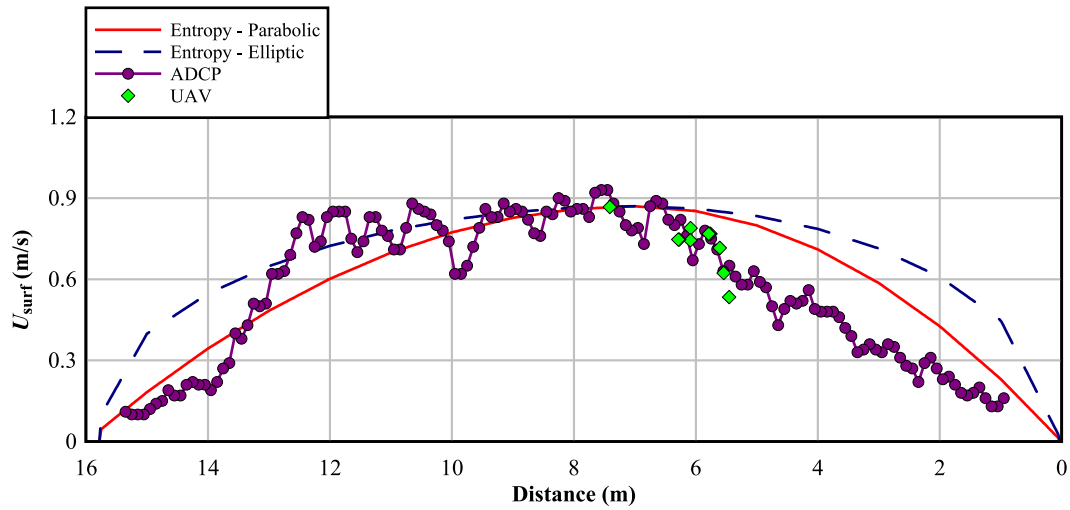

Figure 6. Surface velocity distribution based on parabolic and elliptic distributions, Freiberger Mulde CS3.

certain state under constraints, and does not explicitly deal with individual factors. In other words, at a given cross section, a change in one factor such as sediment concentration leads to self-adjustments of the other parameters in order to keep M or $\Phi(M)$ unchanged. Nonetheless, the sediment-laden flow tends to decrease the magnitude of $\Phi(M)$. In addition, the maximum velocity generally occurs in transverse vertical corresponding to the one where the maximum surface velocity is observed (Corato et al., 2011; Guo & Julien, 2012; Moramarco et al., 2004).

4.2. Discharge Rate and Velocity Distribution

The entropy theory was applied to seven cross sections from the two rivers.

For the first cross section CS1 on the Sajó river near the city of Nagycsécs, Hungary, the maximum surface velocity of $V_{surf\text{-}max} = 1.113$ m/s was detected at the transverse distance of $x = 17$ m based on the UAV data (Figure 4). In addition, the near-surface velocity data of ADCP at the vertical level of 0.25 m below the surface are added to Figure 4, suggesting that the UAV data follow a trend similar to the ADCP data. The difference between UAV and ADCP velocity data can be ascribed to the blank zone of the ADCP equipment. Based on the collected data, $Q = 11.21$ m^3/s, $A = 13.67$ m^2 and $U_m = 0.82$ m/s; consequently, the entropic parameters were $\Phi(M) = 0.732$ and $M = 3.24$. Considering the maximum surface velocity as the only velocity input together with the data of bathymetry, the magnitudes of average velocity, discharge rate, and cross-sectional velocity were predicted. Two scenarios were applied for the distribution of surface velocity in the entropic modeling, parabolic, and elliptic scenarios (Figure 4). Differences between ADCP and UAV velocities at water surface may be ascribed to the blank zone of ADCP measurements. Note that the results of the simulation for the other three cross sections, that is, Sajó CS2, CS3, and CS4, are provided in Supporting Information S1.

Figure 5 depicts the cross-sectional velocity distribution based on both parabolic and elliptic distribution together with ADCP data at the station of CS1. Based on both scenarios, the maximum velocity is encountered in the transverse distance corresponding to the maximum surface velocity; however, the interesting point is the existence of dip for the parabolic scenario suggesting the existence of secondary currents in the flow (Termini & Moramarco, 2020). As demonstrated by Moramarco et al. (2017), for different aspect ratios of channel flow, that is, W/D (where W is the channel width and D is the flow depth), the vertical location of maximum velocity below the water surface is mainly associated with the lateral position of the velocity profiles from the sidewalls.

The 2D velocity data are presented based on ADCP bathymetry without the blank zones (Figure 5c). The same procedure was applied to the Amazon River data (see Bahmanpouri et al., 2022). In the previous work (Bahmanpouri et al., 2022), we presented the results by the entropy approach for considering all surface velocities

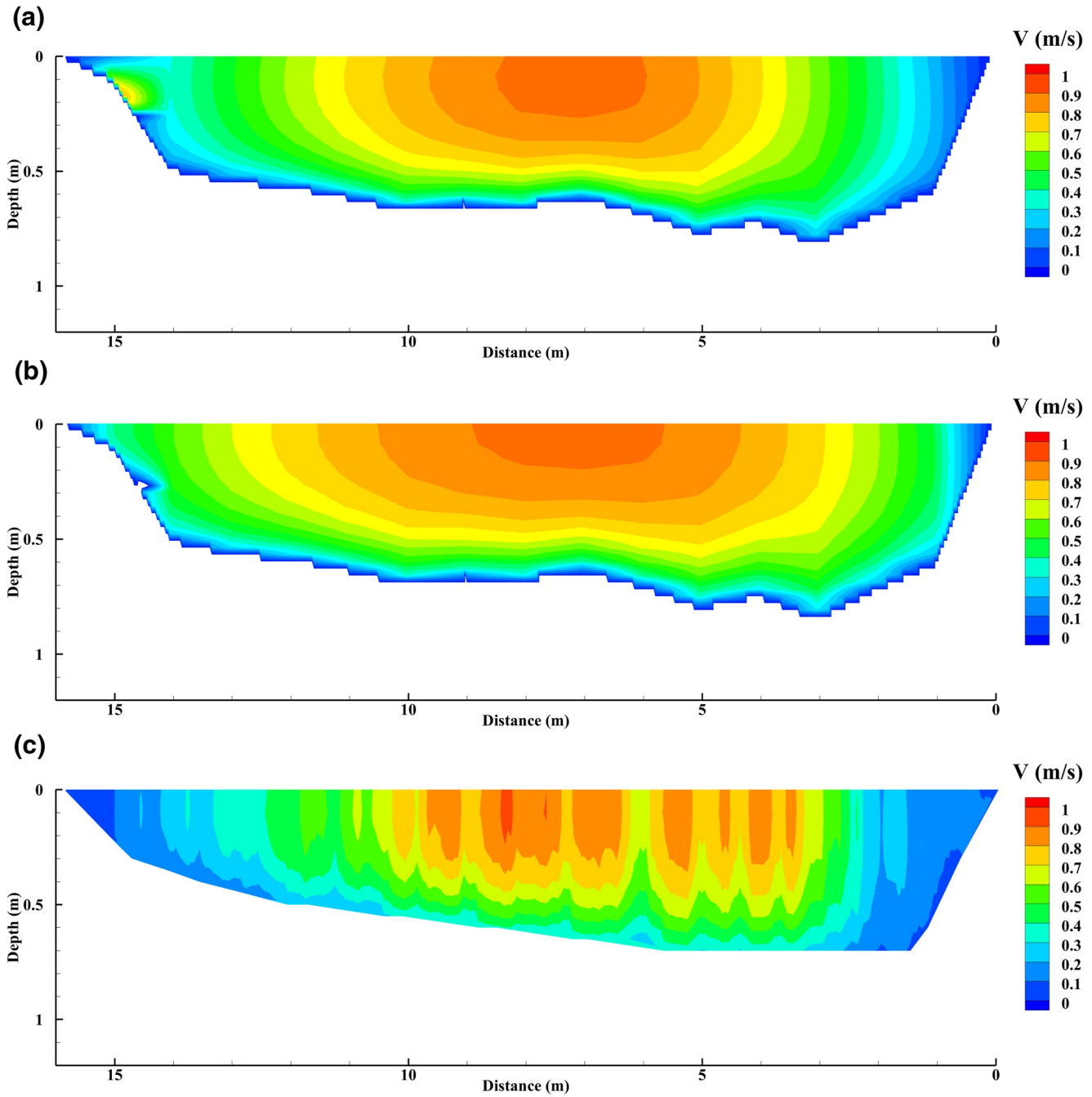

Figure 7. Cross-sectional velocity distribution, Freiberger Mulde CS3, based on uncrewed aerial vehicle bathymetry.

Table 4
The Error Percentage for the Velocity and Discharge Rates

Transect	Scenario for the surface velocity distribution	Average velocity (m/s)		Velocity error (%)	Discharge (m^3/s)		Discharge error (%)
		Measured	Calculated		Measured	Calculated	
Freiberger Mulde CS1	Parabolic	0.57	0.58	1.75	5.60	5.70	1.75
	Elliptic		0.63	10.52		6.19	10.52

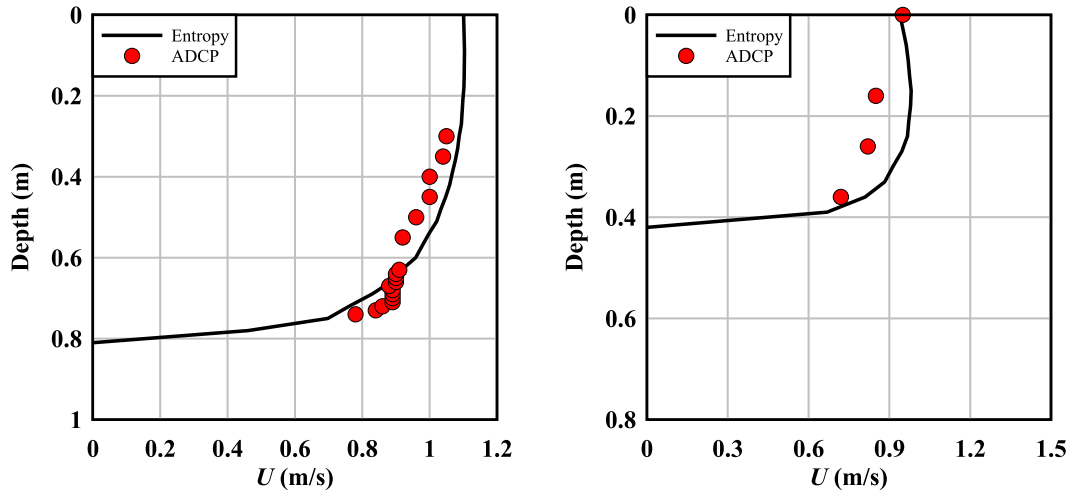

a) Sajó River, CS1, x = 16.0 m b) Freiberger Mulde CS3, x = 5.0 m

Figure 8. Comparison between the observed Acoustic Doppler Current Profilers and predicted entropy magnitudes of the vertical velocity based on the parabolic scenario using uncrewed aerial vehicle measurements at the transverse location of the maximum velocity (y axis).

as input. The results for large rivers, such as the Amazon River, showed how the entropy could estimate 2D velocity with a high accuracy rate.

The entropy modeling based on parabolic and elliptic scenarios resulted in the cross-sectional average velocity of U_m = 0.81 and 0.87 m/s and discharge Q = 11.07 and 11.89 m^3/s, respectively. The error percentage for the velocity and discharge is presented in Table 3.

For the Freiberger Mulde CS1 cross section, the maximum surface velocity is 0.87 m/s at the transverse distance of x = 7.2 m. Based on the observed data, Q = 5.6 m^3/s, A = 9.85 m^2, and U_m = 0.57 m/s. Therefore, according to these data, $\Phi(M)$ = 0.610 and M = 1.37. Figure 6 shows the distribution of collected surface velocity by the UAV procedure together with the two scenarios implemented by the entropy approach. The maximum velocity based on ADCP data is 0.93 m/s, interestingly, in the same transverse location of the maximum velocity (0.87 m/s) by the UAV. The error percentage between the ADCP and UAV maximum velocity magnitudes is 6%.

Figure 7 presents the distribution of cross-sectional velocity based on both parabolic and elliptic surface velocity distributions together with the measurements by ADCP. The dip phenomenon is found in both scenarios, which can be related to the bed topography, the distance from the bank and the aspect ratio as reported by Kundu and Ghoshal (2019). Note that the results of simulation for the other two cross sections, that is, FreibergerMulde CS2 and CS3, are provided in Supporting Information S1. Applying the entropy theory based on parabolic and elliptic scenarios resulted in the cross-sectional average velocity of U_m = 0.58 and 0.63 m/s and discharge Q = 5.70 and 6.19 m^3/s, respectively. The error percentage for the velocity and discharge rates is listed in Table 4.

Figure 8 shows the comparison between the vertical entropy velocity data based on UAV measurements and the available observed ADCP data for the abovementioned cross sections at the transverse location of the maximum velocity (y axis). Table 5 lists the statistical analysis results for the plotted graphs in Figure 8. The coefficient of determination 0.55 < R^2 < 0.86 and the standard error 0.047 < SE < 0.063 suggests a high level of accuracy for the prediction of the velocity field by using the Entropy approach based on the Parabolic scenario.

Table 5
Statistical Analysis for Vertical Velocity Distribution Based on the Parabolic Scenario

River and cross section	Distance from the bank (m)	R^2	Standard error
Sajó River, CS1	16.0	0.86	0.047
Freiberger Mulde CS3	5.0	0.55	0.063

4.3. Discussion

The results suggested that the entropy method applied to UAV's velocity data can model the discharge rate and velocity distribution with an error percentage less than 13%. Regarding the required data for the simulation, first, the entropic parameter Φ(M) was calculated based on ADCP data. In this case,

Table 6
Percentage Error on Velocity and Discharge Estimate Changing the Transverse Location of the Maximum Surface Velocity-Parabolic Scenario

Transect	Change for transverse location (m) of $V_{surf\text{-}max}$	Average velocity (m/s)		Velocity error (%)	Discharge (m^3/s)		Discharge error (%)
		Measured	Calculated		Measured	Calculated	
Freiberger Mulde -CS3	0	0.68	0.65	4.41	6.04	5.77	4.41
	+2	0.68	0.62	8.77	6.04	5.51	8.77
	−2	0.68	0.66	2.81	6.04	5.87	2.81
	+4	0.68	0.63	6.79	6.04	5.63	6.79
	−4	0.68	0.62	8.11	6.04	5.55	8.11

the ADCP data were collected concurrently with the UAV data; thus, the entropy parameters for each section were calculated for the same flow distribution. It is worth considering how the entropy parameters could be estimated for an ungauged flow. Notably, for gauged sites, Φ(M) can be calculated by leveraging the velocity data set considering the set of pairs of mean velocity and max velocity. While, for ungauged sites, the formulation proposed by Moramarco and Singh (2010) can be adopted. This formulation represents a direct relationship between the entropic parameter M and the hydraulic and geometric characteristics of the river section. The previous investigations demonstrated that the magnitude of M based on the formulation would result in a magnitude similar to the one derived from the available velocity data set. According to previous investigations through different rivers, it has been demonstrated that the entropy parameter M is constant for gauged river sections (Corato et al., 2014; Moramarco & Dingman, 2017; Moramarco & Singh, 2010; Xia, 1997). It is worth noting that Moramarco and Singh (2010) showed that $\Phi(M)$ may represent an intrinsic parameter not only of the equipped site but also of the river reach, where sites are located. Regarding the other input data, next, at each cross section, the maximum surface velocity was derived from the UAV. For the present research, bathymetry data from UAV measurements were considered as the input for the entropy approach. The investigation on how to address the same method for high flow conditions, if the bathymetry is not given, would be the scope of the next research work. In that case, we will compare the proposed method using bathymetry retrieved by UAV with the one developed by Moramarco et al. (2019) who estimated the bathymetry from the monitoring of surface velocities across the river site.

Further, the transverse location of the maximum surface velocity was assumed to change very little during high flow conditions (Vyas et al., 2021). Confirming this, Table 6 presents the effect of changing the transverse location of the maximum surface velocity on the estimation of the discharge and mean velocity. The transverse location of the $V_{max\text{-}surf}$ is 5 m and the length of the transect is 18 m. As can be seen, changing the transverse location of the maximum surface velocity up to ±4 m, that is, the middle of the cross section resulted in an error percentage of less than 9%.

Table 7
Percentage Error Applying the Averaged M Magnitudes to Estimate the Mean Velocity and Discharge Rate

Transect	Averaged Φ(M) for each river (all transects)	Averaged M for each river (all transects)	Mean velocity and discharge error (%)–parabolic scenario	Mean velocity and discharge error (%)–elliptic scenario
Sajó CS1	0.68	2.4	3.66	2.42
Sajó CS2			23.10	23.08
Sajó CS3			6.51	21.53
Sajó CS4			7.14	6.52
Freiberger Mulde CS1	0.62	1.5	1.0	8.77
Freiberger Mulde CS2			18.46	12.15
Freiberger Mulde CS3			7.35	2.94

In future work, the method should also be validated by testing M values derived from low flow measurements to predict high flow discharges. Tables 7 and 8 present the application of the entropy parameter based on the averaged magnitude of M for each river and all rivers, respectively. The results based on both parabolic and entropic scenarios demonstrate the error percentage for mean flow velocity and discharge less than 25%.

Regarding the dip phenomenon, it is worth noting that the velocity dip is of particular importance for specifying the flow pattern and the momentum transport processes. Taking into account the velocity dip leads to estimating depth-averaged velocity more accurately, therefore, the estimated discharge would be more robust. The accuracy of estimating the velocity dip by the Entropy approach has been proven in previous works, especially considering the recent study by the authors where they applied the entropy approach to estimate the velocity and discharge through the confluence of Rio Negro and Rio Solimões on the Amazon River as the largest river on the earth in terms of discharge (Bahmanpouri et al., 2022).

Table 8
Percentage Error Applying the Averaged M Magnitude to Estimate the Mean Velocity and Discharge Rate

Transect	Averaged Φ(M) for all rivers (all transects)	Averaged M for each river (all transects)	Mean velocity and discharge error (%)—parabolic scenario	Mean velocity and discharge error (%)—elliptic scenario
Sajó CS1	0.67	2.2	3.65	2.44
Sajó CS2			11.59	26.08
Sajó CS3			6.50	21.52
Sajó CS4			18.38	10.43
Freiberger Mulde CS1			3.75	10.52
Freiberger Mulde CS2			22.46	11.81
Freiberger Mulde CS3			5.87	1.0

Overall, the method can be applied for monitoring high flow at river sites, especially for inaccessible points, just sampling one single surface velocity and bathymetry data by UAV. It should be considered that, for the high flow conditions, the weather condition, for example, rainy and foggy circumstances, especially for high ungauged flows, may affect the surface velocity measurements by radar or UAV. This could be a limitation of the presented method. Further, the possibility of acquiring the data by UAV is a limit of the present method as well as for all noncontact techniques. Nevertheless, the results suggested that the method will lend itself to be operational to deliver real-time mean velocity and discharge especially during high flow, just sampling a singular surface velocity.

5. Conclusion

The entropy approach was applied to predict the velocity distribution and discharge rates in rivers using only one surface velocity measurement as the maximum surface velocity. The UAV-based image processing technique was implemented to obtain the surface velocity distribution along two rivers: the Sajó and the Freiberger Mulde Rivers. Seven cross sections were chosen for the assessment of the model application. The entropic parameter Φ(M) was calculated based on the observed maximum and mean velocity magnitudes extracted by ADCP suggesting a trend for all cross sections with a range of $0.6 < \Phi(M) < 0.75$. The model outputs explored that for some cross sections the vertical elevation of maximum velocity as velocity dip was observed below the water surface mainly due to the existence of secondary flows. The results of the simulation, in terms of the vertical and cross-sectional distribution of the velocity, hinted that the entropy approach can predict the velocity distribution and discharge rates with acceptable accuracy, that is, the error percentage was less than 13% when the parabolic scenario is assumed for the surface velocity distribution. As the main finding, the present research highlighted the potential of the entropy concept to predict velocity and discharge rates, in the presence of a velocity dip, in the rivers based on one surface velocity measurement retrieved by UAV and this insight is of considerable interest for high flow discharge monitoring.

Data Availability Statement

The data set used for the Freiberger Mulde River can be found in https://opara.zih.tu-dresden.de/xmlui/handle/123456789/1405. The ADCP data for Sajó River are available at https://doi.org/10.5281/zenodo.6496919.

Acknowledgments
This work has been supported by Italian National Research Programme PRIN 2017, https://enterprisingprin.eu/ with the project "IntEractions between hydrodyNamics flows and bioTic communities in fluvial Ecosystems: advancement in dischaRge monitoring and understanding of Processes Relevant for ecosystem sustaInability by the development of novel technologies with fIeld observatioNs and laboratory testinG (ENTERPRISING)." AE and LB were supported by the DAAD with funds from the Federal Ministry of Education and Research (BMBF; project ID: 57448822) and the Tempus Public Foundation (project ID: 307670). LB was also supported by the Thematic Excellence Programme (TKP2020-NKA-04) of the Ministry for Innovation and Technology in Hungary. Furthermore, we would like to thank Jens Grundmann for providing the ADCP data at the German rivers.

References

Acharya, B. S., Bhandari, M., Bandini, F., Pizarro, A., Perks, M., Joshi, D. R., et al. (2021). Unmanned aerial vehicles in hydrology and water management–Applications, challenges and perspectives. *Water Resources Research*, *57*(11), e2021WR029925. https://doi.org/10.1029/2021WR029925

Bahmanpouri, F., Barbetta, S., Gualtieri, C., Iannirubertо, M., Filizola, N., Termini, D., & Moramarco, T. (2022). Prediction of river discharges at confluences based on Entropy theory and surface-velocity measurements. *Journal of Hydrology*, *606*, 127404. https://doi.org/10.1016/j.jhydrol.2021.127404

Bandini, F., Olesen, D., Jakobsen, J., Kittel, C. M. M., Wang, S., Garcia, M., & Bauer-Gottwein, P. (2018). Bathymetry observations of inland water bodies using a tethered single-beam sonar controlled by an unmanned aerial vehicle. *Hydrology and Earth System Sciences*, *22*(8), 4165–4181. https://doi.org/10.5194/hess-22-4165-2018

Bertalan, L., Novák, T. J., Németh, Z., Rodrigo-Comino, J., Kertész, Á., & Szabó, S. (2018). Issues of meander development: Land degradation or ecological value? The example of the Sajó River, Hungary. *Water*, *10*(11), 1613. https://doi.org/10.3390/w10111613

Bertalan, L., Rodrigo-Comino, J., Surian, N., Šulc Michalková, M., Kovács, Z., Szabó, S., et al. (2019). Detailed assessment of spatial and temporal variations in river channel changes and meander evolution as a preliminary work for effective floodplain management. The example of Sajó River, Hungary. *Journal of Environmental Management*, *248*, 109277. https://doi.org/10.1016/j.jenvman.2019.109277

Brasington, J., Langham, J., & Rumsby, B. (2003). Methodological sensitivity of morphometric estimates of coarse fluvial sediment transport. *Geomorphology*, *53*(3–4), 299–316. https://doi.org/10.1016/s0169-555x(02)00320-3

Chahrour, N., Castaings, W., & Barthélemy, E. (2021). Image-based river discharge estimation by merging heterogeneous data with information entropy theory. *Flow Measurement and Instrumentation, 81,* 102039. https://doi.org/10.1016/j.flowmeasinst.2021.102039

Chiu, C. L. (1988). Entropy and 2-d velocity in open channels. *Journal of Hydraulic Engineering*, *114*(7), 738–756. https://doi.org/10.1061/(asce)0733-9429(1988)114:7(738)

Chiu, C. L. (1989). Velocity distribution in open channel flow. *Journal of Hydraulic Engineering*, *115*(5), 576–594. https://doi.org/10.1061/(asce)0733-9429(1989)115:5(576)

Chiu, C. L., Hsu, S. M., Tung, & N. C. (2005). Efficient methods of discharge measurements in rivers and streams based on the probability concept. *Hydrological Processes*, *19*(20), 3935–3946. https://doi.org/10.1002/hyp.5857

Chiu, C. L., Jin, W., & Chen, Y. C. (2000). Mathematical models of distribution of sediment concentration. *Journal of Hydraulic Engineering*, *126*(1), 16–23. https://doi.org/10.1061/(asce)0733-9429(2000)126:1(16)

Chiu, C. L., Said, & C. A. A. (1995). Maximum and mean velocities and entropy in open-channel flow. *Journal of Hydraulic Engineering*, *121*(1), 26–35. https://doi.org/10.1061/(asce)0733-9429(1995)121:1(26)

Choo, T. H., Jeong, I. J., Chae, S. K., Yoon, H. C., & Son, H. S. (2011). A study on the derivation of a mean velocity formula from Chiu's velocity formula and bottom shear stress. *Hydrology and Earth System Sciences Discussions,* 8(4), 6419–6442.

Corato, G., Ammari, A., & Moramarco, T. (2014). Conventional point-velocity records and surface velocity observations for estimating high flow discharge. *Entropy*, *16*(10), 5546–5559. https://doi.org/10.3390/e16105546

Corato, G., Moramarco, T., & Tucciarelli, T. (2011). Discharge estimation combining flow routing and occasional measurements of velocity. *Hydrology and Earth System Sciences*, *15*(9), 2979–2994. https://doi.org/10.5194/hess-15-2979-2011

Dal Sasso, S. F., Pizarro, A., & Manfreda, S. (2021). Recent advancements and perspectives in UAS-based image velocimetry. *Drones*, *5*(3), 81. https://doi.org/10.3390/drones5030081

Dietrich, J. T. (2017). Bathymetric structure-from-motion: Extracting shallow stream bathymetry from multi-view stereo photogrammetry. *Earth Surface Processes and Landforms*, *42*(2), 355–364. https://doi.org/10.1002/esp.4060

Ebtehaj, I., Bonakdari, H., Moradi, F., Gharabaghi, B., & Khozani, Z. S. (2018). An integrated framework of extreme learning machines for predicting scour at pile groups in clear water condition. *Coastal Engineering*, *135*, 1–15. https://doi.org/10.1016/j.coastaleng.2017.12.012

Eltner, A., Bertalan, L., Perks, M., Grundmann, J., & Lotsari, E. (2021). Hydro-morphological mapping of river reaches using videos captured with unoccupied aerial systems. *Earth Surface Processes and Landforms,* 46*(*14), 2773–2787. https://doi.org/10.1002/esp.5205

Eltner, A., Mader, D., Szopos, N., Nagy, B., Grundmann, J., & Bertalan, L. (2021). Using thermal and RGB UAV imagery to measure surface flow velocities of rivers. *The International Archives of the Photogrammetry, Remote Sensing and Spatial Information Sciences*, *43*, 717–722. https://doi.org/10.5194/isprs-archives-xliii-b2-2021-717-2021

Eltner, A., Sardemann, H., & Grundmann, J. (2020). Flow velocity and discharge measurement in rivers using terrestrial and unmanned-aerial-vehicle imagery. *Hydrology and Earth System Sciences*, *24*(3), 1429–1445. https://doi.org/10.5194/hess-24-1429-2020

Eltner, A., & Sofia, G. (2020). Structure from motion photogrammetric technique. *Developments in Earth Surface Processes*, *23*, 1–24. https://doi.org/10.1016/B978-0-444-64177-9.00001-1

Fujita, I., Muste, M., & Kruger, A. (1998). Large-scale particle image velocimetry for flow analysis in hydraulic engineering applications. *Journal of Hydraulic Research*, *36*(3), 397–414. https://doi.org/10.1080/00221689809498626

Fulton, J., & Ostrowski, J. (2008). Measuring real-time streamflow using emerging technologies: Radar, hydroacoustics, and the probability concept. *Journal of Hydrology*, *357*(1–2), 1–10. https://doi.org/10.1016/j.jhydrol.2008.03.028

Fulton, J. W., Anderson, I. E., Chiu, C. L., Sommer, W., Adams, J. D., Moramarco, T., et al. (2020). QCam: SUAS-based Doppler radar for measuring river discharge. *Remote Sensing*, *12*(20), 3317. https://doi.org/10.3390/rs12203317

Greco, M., & Moramarco, T. (2016). Influence of bed roughness and cross section geometry on medium and maximum velocity ratio in open-channel flow. *Journal of Hydraulic Engineering*, *142*(1), 06015015. https://doi.org/10.1061/(asce)hy.1943-7900.0001064

Guo, J., & Julien, P. Y. (2012). Application of the modified log-wake law in open-channels. *Journal of Applied Fluid Mechanics*, *1*(2), 17–23. https://doi.org/10.1061/40856(200)200

Huang, W. C., Young, C. C., & Liu, W. C. (2018). Application of an automated discharge imaging system and LSPIV during typhoon events in Taiwan. *Water*, *10*(3), 280. https://doi.org/10.3390/w10030280

Kim, J. S., Baek, D., Seo, I. W., & Shin, J. (2019). Retrieving shallow stream bathymetry from UAV-assisted RGB imagery using a geospatial regression method. *Geomorphology*, *341*, 102–114. https://doi.org/10.1016/j.geomorph.2019.05.016

Kundu, S., & Ghoshal, K. (2019). An entropy based model for velocity-dip-position. *Journal of Environmental Informatics*, *33*(2), 113–128. https://doi.org/10.3808/jei.201600344

Leopold, L. B. (1969). *Sediment transport data for various US rivers*. Personal Communication.

Ljubičić, R., Strelnikova, D., Perks, M. T., Eltner, A., Peña-Haro, S., Pizarro, A., et al. (2021). A comparison of tools and techniques for stabilising UAS imagery for surface flow observations. *Hydrology and Earth System Sciences Discussions*, 1–42. https://doi.org/10.5194/hess-25-5105-2021

Lucas, B. D., & Kanade, T. (1981). *An Iterative image registration technique with an application to stereo vision* (Vol. 81, pp. 674–679).

Matsuba, Y., & Sato, S. (2018). Nearshore bathymetry estimation using UAV. *Coastal Engineering Journal*, *60*(1), 51–59. https://doi.org/10.1080/21664250.2018.1436239

Moramarco, T., Barbetta, S., Bjerklie, D. M., Fulton, J. W., & Tarpanelli, A. (2019). River bathymetry estimate and discharge assessment from remote sensing. *Water Resources Research*, *55*(8), 6692–6711. https://doi.org/10.1029/2018wr024220

Moramarco, T., Barbetta, S., & Tarpanelli, A. (2017). From surface flow velocity measurements to discharge assessment by the entropy theory. *Water*, *9*(2), 120. https://doi.org/10.3390/w9020120

Moramarco, T., & Dingman, S. L. (2017). On the theoretical velocity distribution and flow resistance in natural channels. *Journal of Hydrology*, *555*, 777–785. https://doi.org/10.1016/j.jhydrol.2017.10.068

Moramarco, T., Saltalippi, C., & Singh, V. P. (2004). Estimation of mean velocity in natural channels based on Chiu's velocity distribution equation. *Journal of Hydrologic Engineering*, *9*(1), 42–50. https://doi.org/10.1061/(asce)1084-0699(2004)9:1(42)

Moramarco, T., Saltalippi, C., & Singh, V. P. (2011). Velocity profiles assessment in natural channels during high floods. *Hydrology Research*, *42*(2–3), 162–170. https://doi.org/10.2166/nh.2011.064

Moramarco, T., & Singh, V. P. (2010). Formulation of the entropy parameter based on hydraulic and geometric characteristics of river cross sections. *Journal of Hydrologic Engineering*, *15*(10), 852–858. https://doi.org/10.1061/(asce)he.1943-5584.0000255

Nezu, I., & Rodi, W. (1986). Open-channel flow measurements with a laser Doppler anemometer. *Journal of Hydraulic Engineering*, *112*(5), 335–355. https://doi.org/10.1061/(asce)0733-9429(1986)112:5(335)

Rossi, L., Mammi, I., & Pelliccia, F. (2020). UAV-derived multispectral bathymetry. *Remote Sensing*, *12*(23), 3897. https://doi.org/10.3390/rs12233897

Shi, J., & Tomasi, C. (1994). Good features to track. In *1994 Proceedings of the IEEE conference on computer vision and pattern recognition*, (pp. 593–600). IEEE.

Shinohara, K., & Tsubaki, T. (1959). *On the characteristics of sand waves formed upon beds of the open channels and rivers*, Research Institute of Applied Mechanics, Kyushu University.

Singh, V. P. (2014). *Entropy theory in hydraulic engineering: An introduction*. American Society of Civil Engineers.

Singh, V. P., Sivakumar, B., & Cui, H. (2017). Tsallis entropy theory for modeling in water engineering: A review. *Entropy*, *19*(12), 641. https://doi.org/10.3390/e19120641

Sterling, M., & Knight, D. (2002). An attempt at using the entropy approach to predict the transverse distribution of boundary shear stress in open channel flow. *Stochastic Environmental Research and Risk Assessment*, *16*(2), 127–142. https://doi.org/10.1007/s00477-002-0088-2

Tauro, F., Petroselli, A., & Grimaldi, S. (2018). Optical sensing for stream flow observations: A review. *Journal of Agricultural Engineering*, *49*(4), 199–206. https://doi.org/10.4081/jae.2018.836

Tauro, F., Porfiri, M., & Grimaldi, S. (2014). Orienting the camera and firing lasers to enhance large scale particle image velocimetry for streamflow monitoring. *Water Resources Research*, *50*(9), 7470–7483. https://doi.org/10.1002/2014wr015952

Tauro, F., & Salvatori, S. (2017). Surface flows from images: Ten days of observations from the Tiber River gauge-cam station. *Hydrology Research*, *48*(3), 646–655. https://doi.org/10.2166/nh.2016.302

Termini, D., & Moramarco, T. (2017). Application of entropic approach to estimate the mean flow velocity and manning roughness coefficient in a high-curvature flume. *Hydrology Research*, *48*(3), 634–645. https://doi.org/10.2166/nh.2016.106

Termini, D., & Moramarco, T. (2020). Entropic model application to identify cross-sectional flow effect on velocity distribution in a large amplitude meandering channel. *Advances in Water Resources*, *143*, 103678. https://doi.org/10.1016/j.advwatres.2020.103678

Tsukada, F., Shimozono, T., & Matsuba, Y. (2020). UAV-based mapping of nearshore bathymetry over broad areas. *Coastal Engineering Journal*, *62*(2), 285–298. https://doi.org/10.1080/21664250.2020.1747766

Vanoni, V. A. (1941). *Velocity Distribution in Open Channels, Civil Engineering* (Vol. 11(6), pp. 356–357). ASCE.

Vyas, J. K., Perumal, M., & Moramarco, T. (2021). Entropy based river discharge estimation using one-point velocity measurement at 0.6 D. *Water Resources Research*, *57*(8), e2021WR029825. https://doi.org/10.1029/2021wr029825

Welber, M., Le Coz, J., Laronne, J. B., Zolezzi, G., Zamler, D., Dramais, G., et al. (2016). Field assessment of noncontact stream gauging using portable surface velocity radars (SVR). *Water Resources Research*, *52*(2), 1108–1126. https://doi.org/10.1002/2015wr017906

Williams, R. D., Brasington, J., Hicks, M., Measures, R., Rennie, C. D., & Vericat, D. (2013). Hydraulic validation of two-dimensional simulations of braided river flow with spatially continuous aDcp data. *Water Resources Research*, *49*(9), 5183–5205. https://doi.org/10.1002/wrcr.20391

Woodget, A. S., Carbonneau, P. E., Visser, F., & Maddock, I. P. (2015). Quantifying submerged fluvial topography using hyperspatial resolution UAS imagery and structure from motion photogrammetry. *Earth Surface Processes and Landforms*, *40*(1), 47–64. https://doi.org/10.1002/esp.3613

Xia, R. (1997). Relation between mean and maximum velocities in a natural river. *Journal of Hydraulic Engineering*, *123*(8), 720–723. https://doi.org/10.1061/(asce)0733-9429(1997)123:8(720)

Zinke, P., & Flener, C. (2013). Experiences from the use of unmanned aerial vehicles (UAV) for river bathymetry modelling in Norway. *Vann*, *48*, 351–360.